

The $\text{Fe}^{\text{IV}}\text{-O}^*$ oxyl unit as a key intermediate in water oxidation on the Fe^{III} -hydroxide: DFT predictions

Alexander Shubin¹, Viktor Kovalskii¹, Sergey Ruzankin¹, Igor Zilberberg¹, Valentin Parmon¹, Felix Tomilin², and Paul Avramov³

¹Boreskov Institute of Catalysis SB RAS

²Kirensky Institute of Physics SB RAS

³Kyungpook National University

June 2, 2020

Abstract

The O-O coupling process in water oxidation on the gamma FeOOH hydroxide catalyst is simulated by means of density functional theory using model iron cubane cluster $\text{Fe}_4\text{O}_4(\text{OH})_4$. A key reactive intermediate is proposed to be the $\text{HO-Fe}^{\text{IV}}\text{-O}^*$ oxyl unit with terminal oxo radical formed from vertex $\text{HO-Fe}^{\text{IV}}\text{-OH}$ moiety by withdrawal of proton-electron pair. The O-O coupling goes via water nucleophilic attack on the oxyl oxygen to form the O-O bond with a remarkably low barrier of 11 kcal/mol. This process is far more effective than alternative scenario based on direct interaction of two ferryl $\text{Fe}^{\text{IV}}\text{=O}$ sites (with estimated barrier of 36 kcal/mol) and is comparable with the coupling between terminal oxo center and three-coordinated lattice oxo center (12 kcal/mol barrier). The process of hydroxylation of terminal oxygen inhibits the O-O coupling. Nevertheless, being more effective for ferryl oxygen, the hydroxylation in fact enhances selectivity of the O-O coupling initiated by the oxyl oxygen.

1. Introduction

The hydroxides of transition metals are known to catalyze the water oxidation.^[1] Nowadays, investigations are focused mostly on mixed (Ni,Fe) hydroxide which is extremely effective in this process. The iron moiety of the hydroxide is commonly considered as responsible for overall activity of this material.^[2,3] One of the major open questions in this field is the electron state of “active” iron cation and the detailed mechanism of the O-O coupling. The up-to-date experimental and DFT-computation results are the following. On base of operando Mossbauer spectroscopic studies the $\text{Fe}^{\text{IV}}\text{=O}$ ferryl site of the (Ni,Fe) hydroxide was suggested to be responsible for the water oxidation.^[4] The ferryl site can appear via proton-coupled electron-transfer (PCET) from the $\text{Fe}^{\text{III}}\text{-OH}$ species.^[4] The ferryl model contradicts conclusion by Freibel, Bell, and Nørskov with coauthors^[5] that in $\text{Ni}_{1-x}\text{Fe}_x\text{OOH}$ the actual active site for oxidation of water is Fe^{III} . The latter conclusion was put forward on base of operando X-ray absorption spectroscopy (XAS) combined with high energy resolution fluorescence detection (HERFD) and DFT modeling.^[5] The ferric iron is claimed to occupy under-coordinated octahedral positions appeared on high-index surfaces (0112) or (0114) of NiOOH .^[5] Alternatively, Goddard with coauthors suggested that the $\text{Fe}^{\text{IV}}\text{-O}^*$ species is a key intermediate which determines the activity of the (Ni,Fe) hydroxide in the water splitting.^[6] However, in the latter work the $\text{Fe}^{\text{IV}}\text{-O}^*$ species only assisted the O-O coupling which actually proceeds on the $\text{Ni}^{\text{IV}}\text{-O}^*$ site. Anyway, the idea that the oxyl intermediate is an indispensable participant of the water splitting by hydroxides nicely agrees with suggestion by Siegbahn, that the O-O bond association on natural photosynthetic center necessarily involves

an endergonic formation of oxygen radical.^[7] The only question arises how this intermediate can appear in the hydroxide, taking into account obvious metastability of such radical species.

In our previous work on the O-O coupling, with the use of tetramer cluster model $\text{Fe}_4\text{O}_4(\text{OH})_4$ of the Fe^{III} hydroxide, the ferryl $\text{Fe}^{\text{IV}}=\text{O}$ species was formed from $\text{Fe}^{\text{III}}-\text{OH}$ group via the first PCET.^[8] So-formed ferryl oxygen attacks on the cubane edge forming metastable $\text{Fe}^{\text{III}}-\text{O}^*$ oxyl group with negative spin density on oxygen. It is the spin polarization of the oxyl that makes $\text{Fe}^{\text{III}}-\text{O}^*$ group responsible for further O-O coupling with a low barrier of 12 kcal/mol.^[8] This route happens to be energetically favorable. A competing process blocking this scenario is the hydroxylation of the ferryl center by water molecule to form the $\text{HO}-\text{Fe}^{\text{IV}}-\text{OH}$ moiety. However, the second PCET restores a bare oxo site (having the $\text{HO}-\text{Fe}^{\text{IV}}-\text{O}^*$ or $\text{HO}-\text{Fe}^{\text{V}}=\text{O}$ configuration) capable of the O-O coupling with neighboring cubane corner oxygen. In addition, the presence of hydroxo group in the neighborhood of terminal oxo site creates a possibility of the oxo-hydroxo association at the same Fe center to form the OOH species. So-obtained O-O coupling on a single iron site is though less probable due to a relatively high barrier of 18 kcal/mol.^[8] In this work the O-O coupling is investigated for water nucleophilic attack on the $\text{HO}-\text{Fe}^{\text{IV}}-\text{O}^*$ oxyl site.

As far as the above described formation of the $-\text{O}^*$ or $=\text{O}$ terminal oxo sites are concerned, a question arises whether unavoidable hydroxylation process can deactivate these sites in water solution. One may guess that electrophilic attack of water molecule on oxo sites resulting in the $\text{Fe}^{\text{IV}}=\text{OH}$ and $\text{Fe}^{\text{V}}=\text{OH}$ formation competes with the nucleophilic water attack on the same sites to form hydroperoxo species $\text{Fe}-\text{OOH}$. To answer this question, the DFT comparative modeling of the hydroxylation and oxidation was performed using simple cubane cluster $\text{Fe}_4\text{O}_4(\text{OH})_4$ treated in our previous works.

Model

Active sites of water-oxidation catalysts based on iron hydroxides are believed to have much in common with the structure of gamma- FeOOH hydroxide. The latter consists of the double chain of edge-sharing $\text{Fe}(\text{O},\text{OH})_6$ octahedra. Major structural motif of this Fe-hydroxide is a trimer consisting of iron-centered octahedra (Figure 1). The Fe-O-Fe angle is about 100 degrees, the oxo bridge sites are always three-coordinated, while hydroxo groups couple two or one Fe cation. Monocoordinated hydroxyl can appear only on the vertex of the terminating octahedron and is most probably the subject of the first PCET step initiating various scenarios for the O-O coupling process.

The cubane tetramer $(\text{FeOOH})_4\text{O}$ (Figure 2) was chosen for modeling of the reactive center. Previously this model was proved to be quite useful to study O-O coupling since it allows to simulate oxidation acts and the O-O coupling on the vertex of terminal octahedron in the edge-sharing $\text{M}(\text{O},\text{OH})_6$ ($\text{M}=\text{Co},\text{Fe}$) octahedra chain.^[8-10]

Hosted file

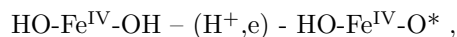
image1.emf available at <https://authorea.com/users/328764/articles/455921-the-feiv-o-oxyl-unit-as-a-key-intermediate-in-water-oxidation-on-the-feiii-hydroxide-dft-predictions>

Figure 1. γ - FeOOH structure: a double chain of edge-sharing $\text{Fe}(\text{O},\text{OH})_6$ octahedra: iron atoms (hidden) are located in the centers of octahedra, oxygen atoms are in vertexes of octahedra (in red), hydrogen centers are in light pink. Dashed lines show the hydrogen bonding between layers of the hydroxide.

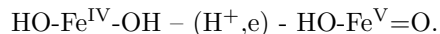
The abstraction of proton and electron from vertex monocoordinated hydroxyl group forms the ferryl group $\text{Fe}^{\text{IV}}=\text{O}$ which can then relatively easily (with a barrier of 12 kcal/mol) couple lattice oxygen at three-coordinated position to form peroxide species. Further release of molecular oxygen from this peroxide species faces no any substantial barriers.^[8] However, far more active terminal oxo center can appear at the second step of proton-electron pair withdrawal via the following steps.^[8] Electrophilic external water molecule attack on the ferryl group can result in the appearance of two hydroxyls instead of ferryl group:



The removal of electron-proton pair from one of these hydroxyls forms another bare terminal oxygen of the oxyl or ferryl type at the same iron cation:



or



So-formed group possessing oxyl configuration $\text{HO-Fe}^{\text{IV}}\text{-O}^*$ can be apparently quite reactive toward the O-O coupling process due to high value of β -spin density on it.

With these reasons in mind, the model reactive center was chosen to be above mentioned cubane cluster having terminal oxo and hydroxo ligands at the corner (Figure 2). The total electron spin projection of this cluster is set to 9 on the base of the following data: for previously considered tetramer $\text{Fe}_4\text{O}_4(\text{OH})_4$ the lowest total energy corresponds to maximal total spin of 10 meaning ferromagnetic coupling of metal centers with spin of $5/2$.^[8] Removal of first proton-electron pair from hydroxyl group to form terminal ferryl oxo center decreases total spin to $19/2$. Hydroxylation of ferryl center to form the $\text{HO-Fe}^{\text{IV}}\text{-OH}$ moiety followed by the second proton-electron pair removal from hydroxyl group at Fe^{IV} further decreases total spin to 9. Formally, the electron configuration for obtained iron core is most likely $\text{Fe}^{\text{V}}(\text{S}=3/2)\text{Fe}^{\text{III}}(\text{S}=5/2)\text{Fe}^{\text{III}}(\text{S}=5/2)\text{Fe}^{\text{III}}(\text{S}=5/2)$ or $\text{Fe}^{\text{IV}}(\text{S}=2)\text{Fe}^{\text{III}}(\text{S}=5/2)\text{Fe}^{\text{III}}(\text{S}=5/2)\text{Fe}^{\text{III}}(\text{S}=5/2)$ with the reactive iron Fe1 being in competing Fe^{V} (in ferryl group) or Fe^{IV} (in oxyl group) state corresponding formally to $\text{S}=0$ or $\text{S}=1/2$ on terminal oxo site, respectively.

Hosted file

image2.emf available at <https://authorea.com/users/328764/articles/455921-the-feiv-o-oxyl-unit-as-a-key-intermediate-in-water-oxidation-on-the-feiii-hydroxide-dft-predictions>

Figure 2. Gas-phase cubane model of the FeOOH hydroxide with the HO-Fe-O moiety (black for Fe, red for O, grey for H). The insert on the right shows the atom-numbering scheme. The listed numbers with three and two decimal digits show the distances in Å (in black), and Mulliken spin density (in blue) on atoms, respectively. There are given the spin projection S_z used for calculation and obtained expectation value of spin-squared operator $\langle \mathbf{S}^2 \rangle$ for Kohn-Sham determinant. The same convention is applied for all figures below.

2. Computational details

All calculations were performed at UB3LYP/6-311G++(d,p) level of theory with ultrafine integration grid within the framework of the Gaussian09 package.^[11] For initial $\text{Fe}_4\text{O}_4(\text{OH})_4$ cluster with parallel spins on all iron centers the solution for the spin projection of 10 appears to have minimal energy among all possible iron spins configurations. Ferromagnetic coupling of spins on metal centers seems to be a consequence of cubic geometry of tetramer $\text{Fe}_4\text{O}_4(\text{OH})_4$ having right angles Fe-O-Fe in a perfect agreement with the prediction of negligible superexchange for the $\text{Fe}^{3+}\text{-O}^{2-}\text{-Fe}^{3+}$ linkage at the Fe-O-Fe angle of 90° .^[12,13] For selected most important complexes the presence of water solvent was accounted within Polarizable Continuum Model (PCM) using the integral equation formalism (IEFPCM)^[14] which is the default SCRF method in Gaussian09. In order to get some insight into the electron state of the oxygen and iron centers participating in the interaction with water molecules, the core 1s energies were estimated by the lowest Kohn-Sham molecular orbitals. These energies allow to indirectly interpret the change of electron density on particular center via the shift of the 1s energy of this center: the lower core level, the less electron density.

3. Results and discussion

Oxidation of water

True O-O coupling takes place in case of the water molecule nucleophilic attack on the terminal oxyl oxygen. The process starts from the formation of hydrogen bonds between water molecule and the OH ligand of reactive iron center (Figure 3a). Two simultaneous steps take place: *i*) transfer of proton from water to hydroxyl ligand at the Fe1 site and *ii*) coupling of remaining OH group with terminal oxyl oxygen. In transition state of this process the terminal oxygen changes its spin density from -0.83 to 0.23 reflecting a change of electron configuration of the HO-Fe-O moiety (Figure 3b). Correspondingly, water oxygen acquires a distinct negative spin density of -0.55 becoming a radical-like species (Figure 3b). This apparently facilitates the electron pairing to form closed shell in forming the OOH group at reactive iron Fe1.

The barrier of 11 kcal/mol for splitting of water oxo center at the oxyl site looks amazingly low in comparison with barriers of 22-43 kcal/mol for direct coupling of oxo centers on neighboring iron centers as found in our previous work (Figure 5-7 in ref. [8]). Especially interesting is the comparison with the OOH group formation (with a barrier of 18 kcal/mol) at the same site without participation of external water molecule (Figure 4 in ref. [8]). Present work reveals an effect of upcoming water molecule, which catalyzes this process dropping the barrier by 7 kcal/mol. Before water splitting an initial combination of oxidation states for cluster with oxyl oxygen is formally $\text{Fe}_4(\text{IV},\text{III},\text{III},\text{III})$ (Figure 3a). Under the water molecule attack it becomes $\text{Fe}_4(\text{II},\text{III},\text{III},\text{III})$ as seen from dropping of spin density on Fe1 from 3.40 to 2.83 (Figures 3a, c) and corresponding rising of the core energy $\epsilon_{1s}(\text{Fe})$ by 2.2 eV (Table S1) implying substantial “back” transfer of electron density from oxo and hydroxo ligands into iron center.

One might suspect that a low barrier for the O-O coupling obtained for five-coordinated reactive iron site Fe1 is an artifact resulting from the absence of sixth ligand. To clarify that an additional water molecule was attached to Fe1 to form six-coordinated iron center of cubane (Figure S2a) and the process has been modeled again. It appears that the water ligand remains untouched by the process. Therefore, it is not surprising that the barrier of the O-O coupling decreases by only 2 kcal/mol, in fact coinciding with the results for coordinatively unsaturated iron site. This reveals the evidence that the actual proton transfer between upcoming water molecule and hydroxo group and simultaneous O-OH coupling is governed mostly by the electron state of Fe1 and the terminal oxyl oxygen. Moreover, the barrier seems to be determined by the ability of reactive iron Fe1 cation and its immediate three oxo neighbors (connecting Fe1 to other metal sites) to adopt formally two electrons from terminal oxo center and hydroxo groups becoming OOH and water ligands. Therefore, water solvation could not bring noticeable contribution into this process.

Hosted file

image3.emf available at <https://authorea.com/users/328764/articles/455921-the-feiv-o-oxyl-unit-as-a-key-intermediate-in-water-oxidation-on-the-feiii-hydroxide-dft-predictions>

Figure 3. Energy diagram for nucleophilic attack of water molecule on oxyl oxygen in HO-Fe^{IV}-O* moiety to form Fe-OOH at the Fe1 site : (a) initial complex containing adsorbed water molecule, (b) transition-state complex, and (c) resulting hydroxylated complex. Integer numbers in energy diagram show the total energy differences (in kcal/mol).

Hydroxylation

Terminal oxyl oxygen disappears under the electrophilic water attack since the oxygen is exposed to the proton moiety of the water molecule. The only way to arrange such an approach of water molecule is to adsorb it first on the neighboring metal cation (Figure 4a) to avoid undesired interaction with hydroxyl group on Fe1. When oxyl oxygen in the HO-Fe^{IV}-O* moiety abstracts proton from adsorbed water molecule, two hydroxyl groups appear on metal sites (Figure 4c), rather than the Fe-OH moiety and free OH radical as it might be expected for the water oxidation route by analogy with the abstraction of hydrogen from methane on oxyl oxygen producing methyl radical.^[15] Therefore, the low barrier process (9 kcal/mol) has to be assigned to the dissociative adsorption or hydroxylation.

The same is true for electrophilic water attack on ferryl oxygen (Figure 5). For the latter case, the abstraction of hydrogen by ferryl oxygen to form two hydroxyl anions goes through even a lower barrier of 4 kcal/mol

(Figure 5). This might be explained by more nucleophilic nature of ferryl oxygen preferable for proton abstraction. Nucleophilicity of ferryl and oxyl oxo sites can be compared by means of the difference between the energy of their calculated $1s(O)$ level. The latter is 1.2 eV lower than the former, which means less negatively charged oxyl oxygen (Table S1). This explanation is in line with intuitive picture of the oxyl oxygen appearance via “back” transfer of electron from ferryl-state oxygen to iron center. Mulliken charges on oxyl and ferryl oxygen agree surprisingly good with the core level energies.

Although the hydroxylation of oxyl oxygen in the $HO-Fe^{IV}-O^*$ group and neighboring Fe^{III} center has to form two chemically equivalent sites having two hydroxo ligands (Figure 4c), their spin density (and so the oxidation state) remains different at all stages of process (Figure 4). However, a crucial change takes place for the Fe2 site despite the fact that is not directly involved in the process. The spin density at Fe2 drops from 4.21 to 3.40. Taking into account that energies of $1s$ level for the iron centers with spins 3.34 (Fe1) and 3.40 (Fe2) (Figure 4c) are equal within 0.01 eV (Table S1), one might guess that the oxidation state of Fe2 is 4+ coinciding with that for Fe1 (Figure 4a). What is interesting, initial oxyl containing cubane has oxidation states $Fe_4(IV,III,III,III)$ (Figure 4a). Therefore, the hydroxylation changes this configuration to $Fe_4(IV,IV,III,III)$ (Figure 4c) implying delocalization of spin over the oxo bridges. This result reveals unusual effect that the dissociative adsorption of water (which normally proceeds without any electron transfer) on cluster affects the oxidation states of connected iron centers. This effect is certainly connected with the partial disruption of cubane structure as seen from the elongation of one of edges by almost 1 Å (Figure 4c). In case of hydroxylation of the ferryl-oxo cubane the oxidation scheme is $Fe_4(IV,IV,III,III)$ from the beginning at each steps of the process (Figure 5).

Worthwhile noting that the account of solvation does not change much the structure and relative energies of above given process of water dissociation. For the processes (in both oxyl and ferryl cases) modeled without such account, the barrier is only 1-2 kcal/mol larger than that for the model with solvation (Figure S4-S5).

Hosted file

image4.emf available at <https://authorea.com/users/328764/articles/455921-the-feiv-o-oxyl-unit-as-a-key-intermediate-in-water-oxidation-on-the-feiii-hydroxide-dft-predictions>

Figure 4. Water electrophilic attack on oxyl oxygen (with negative Mulliken spin density of -0.82) within the $HO-Fe^{IV}-O^*$ site at Fe1: (a) initial complex containing adsorbed water molecule, (b) transition-state complex, and (c) resulting hydroxylated complex.

Hosted file

image5.emf available at <https://authorea.com/users/328764/articles/455921-the-feiv-o-oxyl-unit-as-a-key-intermediate-in-water-oxidation-on-the-feiii-hydroxide-dft-predictions>

Figure 5. Water electrophilic attack on ferryl $HO-Fe^V=O$ site: (a) initial complex containing adsorbed water molecule, (b) transition-state complex, and (c) resulting hydroxylated complex.

4. Conclusions

In the present work the cubane cluster $OFe_4(\mu-O)_4(OH)_5$ was used to model the O-O coupling versus hydroxylation of the reactive terminal oxo center on the iron-containing oxyhydroxides by means of DFT with solvent account. The following results are obtained.

- The water nucleophilic attack on the oxyl oxygen to form the OOH group proceeds with a remarkably low barrier of 11 kcal/mol.
- The water electrophilic attack on the reactive corner site results in an easy hydroxylation of both types of oxo sites ($HO-Fe^{IV}-O^*$ and $HO-Fe^V=O$).
- The activation barrier for hydroxylation of oxyl oxygen is predicted to be 9 kcal/mol, while in the case of ferryl oxygen the barrier is as low as 4 kcal/mol.

The barrier estimations allow one to conclude that the O-O coupling and hydroxylation and are equally

probable. From two forms of terminal oxo center the ferryl one is preferred for hydroxylation and is less preferred for O-O coupling. Therefore, the hydroxylation in fact enhances selectivity of the O-O coupling on the oxyl-oxygen centers.

References

1. B. M. Hunter, H. B. Gray and A. M. Müller, *Chem. Rev.* ,**2016** , 116, 14120–14136.
2. M. G. Walter, E. L. Warren, J. R. McKone, S. W. Boettcher, Q. Mi, E. A. Santori and N. S. Lewis, *Chem. Rev.* , **2010** , 110, 6446–6473.
3. Y. F. Li and A. Selloni, *ACS Catal.* , **2014** , 4, 1148–1153.
4. J. Y. C. Chen, L. Dang, H. Liang, W. Bi, J. B. Gerken, S. Jin, E. E. Alp and S. S. Stahl, *J. Am. Chem. Soc.* , **2015** , 137, 15090–15093.
5. D. Friebel, M. W. Louie, M. Bajdich, K. E. Sanwald, Y. Cai, A. M. Wise, M. J. Cheng, D. Sokaras, T. C. Weng, R. Alonso-Mori, R. C. Davis, J. R. Bargar, J. K. Nørskov, A. Nilsson and A. T. Bell, *J. Am. Chem. Soc.* , **2015** , 137, 1305–1313.
6. H. Xiao, H. Shin and W. A. Goddard, *Proc. Natl. Acad. Sci. U. S. A.* , **2018** , 201722034.
7. P. E. M. Siegbahn, *Acc. Chem. Res.* , **2009** , 42, 1871–80.
8. A. A. Shubin, S. P. Ruzankin, I. L. Zilberberg, O. P. Taran and V. N. Parmon, *Chem. Phys. Lett.* , **2015** , 619, 126–132.
9. M. J. Filatov, G. L. Elizarova, O. V. Gerasimov, G. M. Zhidomirov and V. N. Parmon, *J. Mol. Catal.* , **1994** , 91, 71–82.
10. L.-P. Wang and T. Van Voorhis, *J. Phys. Chem. Lett.* ,**2011** , 2, 2200–2204.
11. M. J. Frisch, G. W. Trucks, H. B. Schlegel, G. E. Scuseria, M. A. Robb, J. R. Cheeseman, G. Scalmani, V. Barone, B. Mennucci, G. A. Petersson, H. Nakatsuji, M. Caricato, X. Li, H. P. Hratchian, A. F. Izmaylov, J. Bloino, G. Zheng, J. L. Sonnenberg, M. Hada, M. Ehara, K. Toyota, R. Fukuda, J. Hasegawa, M. Ishida, T. Nakajima, Y. Honda, O. Kitao, H. Nakai, T. Vreven, J. Montgomery, J. A., J. E. Peralta, F. Ogliaro, M. Bearpark, J. J. Heyd, E. Brothers, K. N. Kudin, V. N. Staroverov, R. Kobayashi, J. Normand, K. Raghavachari, A. Rendell, J. C. Burant, S. S. Iyengar, J. Tomasi, M. Cossi, N. Rega, N. J. Millam, M. Klene, J. E. Knox, J. B. Cross, V. Bakken, C. Adamo, J. Jaramillo, R. Gomperts, R. E. Stratmann, O. Yazyev, A. J. Austin, R. Cammi, C. Pomelli, J. W. Ochterski, R. L. Martin, K. Morokuma, V. G. Zakrzewski, G. A. Voth, P. Salvador, J. J. Dannenberg, S. Dapprich, A. D. Daniels, Ö. Farkas, J. B. Foresman, J. V. Ortiz, J. Cioslowski and D. J. Fox,**2013** .
12. P. W. Anderson, *Phys. Rev.* , **1950** , 79, 350–356.
13. M. A. Gilleo, *Phys. Rev.* , **1958** , 109, 777–781.
14. J. Tomasi, B. Mennucci and R. Cammi, *Chem. Rev.* ,**2005** , 105, 2999–3093.
15. V. Kovalskii, A. Shubin, Y. Chen, D. Ovchinnikov, S. P. Ruzankin, J. Hasegawa, I. Zilberberg and V. N. Parmon, *Chem. Phys. Lett.* ,**2017** , 679, 193–199.